FEBS Letters 580 (2006) 6039–6046

Localization of Kv1.5 channels in rat and canine myocyte sarcolemma

Jodene Eldstrom[a,*], David R. Van Wagoner[b], Edwin D. Moore[a], David Fedida[a]

[a] *Department of Anesthesiology, Pharmacology and Therapeutics, University of British Columbia, 2350 Health Sciences Mall, Vancouver, BC, Canada V6T 1Z3*

[b] *Department of Cardiology, Cleveland Clinic Foundation, Cleveland, OH 44195, USA*

Received 13 September 2006; accepted 27 September 2006

Available online 12 October 2006

Edited by Maurice Montal

Abstract **Voltage-gated potassium (Kv) channel subtypes localize to the plasma membrane of a number of cell types, and the sarcolemma in myocytes. Because many signaling molecules concentrate in subdomains of the plasma membrane, the localization of Kv channels to these sites may have important implications for channel function and regulation. In this study, the association of the voltage-gated potassium channel Kv1.5 with a specific subtype of lipid rafts, caveolae, in rat and canine cardiac myocytes has been investigated. Interactions between caveolin-3 and β-dystroglycan or eNOS, as well as between Kv1.5 and α-actinin were readily detected in co-immunoprecipitation experiments, whereas no association between Kv1.5 and caveolin-3 was evident. Wide-field microscopy and deconvolution techniques revealed that the percent co-localization of Kv1.5 with caveolin-3 was extremely low in atrial myocytes from rat and canine hearts (8 ± 1% and 12.2 ± 2%, respectively), and limited in ventricular myocytes (11 ± 4% and 20 ± 3% in rat and canine, respectively). Immunoelectron microscopic imaging of rat atrial and ventricular tissues showed that Kv1.5 and caveolin-3 labeling generally did not overlap. In HEK293 cells stably expressing the channel, Kv1.5 did not target to the low buoyant density raft fraction along with flotillin but instead fractionated along with the non-raft associated transferrin receptor. Taken together, these results suggest that Kv1.5 is not present in caveolae of rat and canine heart.**

Keywords: Kv channel; Lipid rafts; Caveolin; Cardiac myocytes

1. Introduction

Studies in cultured mouse *ltk*-cells [1,2], tsA201 cells, mouse brain [3], pancreatic β-cells [4] and Jurkat T-lymphocytes [5] have found several subtypes of voltage-gated potassium (Kv) channels to be sorted to specialized domains in the plasma membrane called lipid rafts. Because lipid rafts are thought to concentrate signaling molecules for more efficient transduction, this targeting may provide a mechanism for differential regulation of targeted channels. A lipid raft subgroup of particular interest in myocytes is caveolae, which are flask-like invaginations of the surface membrane containing the muscle-specific caveolin-3.

Caveolae are characterized by a coat of caveolin-1 or caveolin-3, and a third type of caveolin, caveolin-2, although studies of the subtypes have indicated that caveolin-2 requires co-expression of caveolin-1 or -3 in order to express in the plasma membrane [6]. Mice lacking caveolin-3 show a defective T-tubule system and changes in the dystrophin–glycoprotein complex distribution associated with the loss of caveolae in skeletal muscle [7] and a progressive hypertrophic cardiomyopathy [8]. Overexpression of caveolin-3 leads to severe cardiac tissue damage and fibrosis and a prolonged QRS duration in transgenic mice [9]. Several proteins are associated with these domains including c-Src, G-protein α-subunits [10], H-Ras [11] and eNOS [12] as well as various receptors [13,14] including the β_2-adrenergic receptor [15]. Caveolae have been implicated in the regulation of targeted signal cascades (reviewed in [16,17]), in clathrin-independent endocytosis (reviewed in [18]), calcium signaling (reviewed in [19]), and in cholesterol trafficking (reviewed in [17]). Caveolins may also stabilize the caveolar invagination and slow the dynamin-dependent internalization process [18].

Here, we have studied the molecular correlate of I_{KUR}, Kv1.5 [20,21], a channel that is highly expressed in human atrial myocytes [20]. I_{KUR} is an important contributor to the repolarization phase of the atrial action potential, but appears to have little electrophysiological role in the ventricle. Therefore, Kv1.5 has generated significant interest as an atrial-specific target for the treatment of atrial fibrillation [22,23]. It would be of great interest to know whether Kv1.5 localizes to lipid rafts in normal adult mammalian cardiac myocytes where the proteins are expressed at physiological levels, and more specifically whether it localizes in caveolae in association with caveolin-3.

Significantly, many of the same signaling molecules known to localize in caveolae affect Kv1.5. Kv1.5 can be modulated by protein kinases such as Src [24] and PKA [25] and I_{KUR} is influenced by β_2-adrenergic stimulation [26]. Localization to caveolae appears to be a dynamic process with several receptors, such as the β_2-adrenergic receptor [27] and the muscarinic acetylcholine receptor [28] entering caveolae upon agonist stimulation; receptors such as the adenosine A_1 receptor [13] translocate out of caveolae upon activation. It is conceivable that regulation of Kv1.5 could similarly involve regulated localization of the channel or localization of molecules that regulate the channel. Intriguingly, Kv1.5 may be inactivated by phosphorylation [24], and Src kinase, which has been shown to regulate Kv1.5 activity, appears to translocate out of caveolae upon activation [29].

In the study reported here, we have used biochemical methods, wide-field microscopy combined with deconvolution

*Corresponding author.
E-mail address: fedida@interchange.ubc.ca (J. Eldstrom).

0014-5793/$32.00
doi:10.1016/j.febslet.2006.09.069

techniques and immunoelectron microscopy to investigate the spatial localization of Kv1.5 and caveolins in rat and canine cardiac myocytes. We show that, from myocyte lysates, Kv1.5 does not coimmunoprecipitate with the major caveolar coat protein, caveolin-3, nor does the channel co-localize appreciably with this marker for caveolae. Also, unlike caveolin, which sediments in lipid raft fractions, Kv1.5 sediments into non-lipid raft fractions from cardiac and cultured HEK293 cell membranes.

2. Materials and methods

2.1. Preparation of canine heart lysates

Canine atrial and ventricular tissue was obtained from heartworm-negative mongrel dogs (20–30 kg) as previously described [23]. Dogs were anesthetized with intravenous pentobarbital sodium (30 mg/kg) and fentanyl citrate (15 μg/kg) and placed on positive-pressure ventilation. A catheter was inserted into the right femoral artery, and the dogs were exsanguinated. A left lateral thoracotomy was performed through the fifth intercostal space, and the heart was arrested. All surgical procedures and experimental protocols were approved by the Cleveland Clinic Foundation Institutional Animal Care and Use Committee (Cleveland, OH).

For rat samples, adult male Wistar rats weighing between 250 and 300 g were killed with an overdose of sodium pentobarbital (65 mg/kg body weight) and 2 U of heparin sodium USP. These procedures were approved by the UBC Committee on Animal Care (Vancouver, BC). The freshly excised ventricular or atrial tissue was added to ice cold non-denaturing lysis buffer and homogenized as described in [23] and lysates were processed as described previously [30]. Following transfer to PVDF membranes the samples were probed with either rabbit anti-Kv1.5 (1:10000; developed in our laboratory [23], mouse anti-caveolin-3, rabbit anti-caveolin-1, mouse anti-β-dystroglycan (1:10000; BD Bioscience), mouse anti-caveolin-2 (1:5000; BD Bioscience), rabbit anti-eNOS (1:5000; Chemicon Int.), or mouse anti-actinin (1:10000, Sigma). HRP conjugated goat anti-rabbit IgG or sheep anti-mouse (1:10000; Jackson Laboratories) were used as secondary antibodies for detection using a chemiluminescent reagent (Western Lightning, Perkin–Elmer).

2.2. Myocyte preparation

Atrial myocytes were dissociated from canine atrial specimens using a chunk dissociation technique [23], and rat myocytes using methods described by Scriven et al. [31] except that when the hearts began to soften, atria were removed separately, and triturated in physiological saline. Canine ventricular myocytes were isolated using the segmental coronary artery perfusion technique [32].

2.3. Immunolabeling and wide-field microscopy

Myocytes, stored in PBS-azide solution after fixation [23], were plated onto poly-L-lysine coated coverslips. For rat myocytes, after blocking, the rabbit polyclonal Kv1.5 primary antibody, diluted in antibody buffer (150 mM NaCl, 15 mM Na_3 Citrate, 3 mM NaN_2 with 1% BSA, 2% (v/v) goat serum and 0.05% (v/v) Triton X), was incubated with the cells first, followed by secondary antibody conjugated with fluorescein isothiocyanate (FITC); then the mouse anti-caveolin-3 monoclonal antibody, followed by a Texas Red secondary antibody. All primary antibodies were incubated overnight; the secondary antibodies were incubated for 1.5 h. Immunolabeling of canine samples was as previously reported [23].

Images were acquired using a Nikon Diaphot 200 inverted microscope. 2D images (magnification, ×600) acquired from a thermoelectrically-cooled CCD camera through the whole cell at 0.25 μm intervals were stacked into 3D images after subtraction of dark current and background, and deconvolved using an empirically determined point-spread-function [31]. Dual fluorescence beads were added to mounting media and used to guide the overlapping of two images acquired at different emission wavelengths. The threshold intensity was applied to remove the noise on images before analyzing the data. Data were presented as means ± S.E.M. *N* refers to the number of cells collected from 3 to 4 animals.

2.4. Preparation of Tokuyasu sections and immunolabeling

After overdose with Pentobarbitol, rats were perfused via the right ventricle with 10 ml of cold PBS using a peristaltic pump before a 10 min perfusion with 4% paraformaldehyde in 0.1 M phosphate buffer (PB). After removal of the heart, the tissue was cut into smaller sections under fixative. After a 50 mM buffered glycine aldehyde block, the small tissue pieces were infiltrated (37 °C with constant rotation) with increasing concentrations of buffered gelatin up to 12% gelatin. The gelatin was allowed to harden at 4 °C and the tissue pieces were cut out and placed into 2.3 M sucrose in 0.1 M PB and allowed to rotate overnight at 4 °C. Cryoprotected tissue was mounted onto cryopins and frozen in liquid nitrogen. Thin sections were cut using a Leica Ultracut T (Leica Microsystems, Canada) and a 35° cryo-diamond knife (Diatome). Ribbons were picked up in a drop of 1% methyl cellulose and 1.15 M sucrose, allowed to thaw on copper grids and immediately placed section side down onto a plate of hardened 2% buffered gelatin for short-term storage.

For immunolabeling of Tokuyasu sections (adapted from [33]), grids were floated on drops of: (a) 0.1 M PB (20 min); (b) 1% glycine (5 min); (c) PB (3 × 3 min); (d) PBS/3% BSA (10 min); (e) mouse anti-caveolin-3 and rabbit anti-Kv1.5 antibody diluted 1/10 and 1/120 in PBS/3% BSA (30 min); (f) PB (5 × 3 min); (g) PBS/3% BSA (5 min); (h) anti-mouse IgG-10 nm gold (Sigma) and anti-rabbit IgG-5 nm gold (20 min; Ted Pella Inc.); (i) PB (5 × 3 min); (j) dH_2O (10 × 3 min); (k) 2:8 ratio of 2% uranyl acetate (UA) to 4% methyl cellulose (MC) on ice (5 min), excess UA/MC was wicked away and samples air dried. Images were acquired using a Hitachi H7600 Transmission Electron Microscope.

2.5. Sucrose gradient raft fractionation

HEK293 cells, stably expressing Kv1.5, from five ~95% confluent T75 Culture Flasks were suspended in 5 ml of ice-cold homogenization buffer (150 mM NaCl, 20 mM Na_2PO_4, 2 mM NaH_2PO_4, 20% (w/v) glycerol) and homogenized in a Dounce Homogenizer on ice. The homogenate was then sonicated (Vibra-Cell Ultrasonic Processor, Sonics and Materials Inc.) 3–30 s pulses with 1 min cooling periods between. The homogenate was then centrifuged at 10000 rpm for 11 min at 4 °C (SW55 Rotor) to pre-clear the sample of nuclei and debris. The supernatant was then centrifuged at 55000 rpm for 33 min at 4 °C to isolate the membrane fraction. The supernatant from this spin was saved as the cytosolic fraction. The membrane pellet was resuspended and incubated 15 min in ice-cold solubilization buffer (25 mM Mes pH 6.5, 150 mM NaCl, 1% Triton X-100 plus protease inhibitors). Solubilized membrane (2.0 ml) was transferred to a 12 ml ultracentrifuge tube and 2.0 ml of ice-cold 80% sucrose in Mes-Buffered Saline (MBS; 25 mM Mes pH 6.5, 150 mM NaCl) was added and mixed thoroughly. Four millilitres of 30% sucrose in MBS was layered gently on top of the first layer and then 4 ml of 5% sucrose in MBS above the 30%. The samples were then spun at 35000 rpm for 12.5 h at 4 °C in a SW41 Ti Rotor. Twelve 1-ml fractions were collected from the top of the gradient and the pellet was washed extensively with PBS before being solubilized in MBS with 2% SDS. The re-suspended pellet was centrifuged at 21000 × *g* and the supernatant run with the rest of the gradient fractions on a 10% SDS–PAGE gel as the fractionation pellet (FP). The fractions were probed with mouse anti-human transferrin receptor (Zymed Laboratories), mouse anti-flotillin-1 (BD Transduction) and rabbit anti-Kv1.5 antibodies.

3. Results

3.1. Kv1.5 and caveolin-3 are present in rat and canine cardiac tissue

We have used several approaches to investigate the interaction of Kv1.5 and caveolins in cardiac myocytes. Since caveolin-3 is found predominantly in muscle tissue [34], we initially employed Western blotting to assay for Kv1.5, caveolin-2, and caveolin-3 in samples prepared from rat and canine atrium and ventricle (Fig. 1). The rat atrium and ventricular samples are shown to the left of the canine samples and Kv1.5 is apparent as a faint band of approximately 83 kDa in all lanes. In contrast, caveolin-3 in the middle panels was highly expressed in all samples. Caveolin-2 (Fig. 1, bottom) could be detected only in

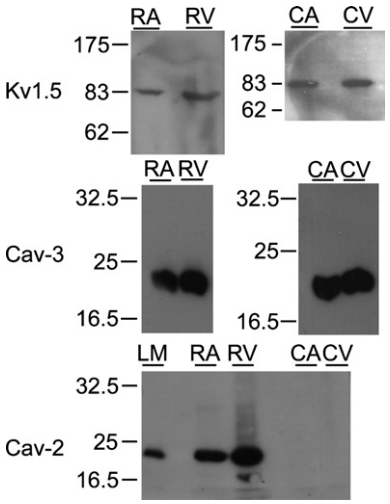

Fig. 1. Kv1.5 and caveolin-3 are expressed in rat and canine atrial and ventricular tissues. Homogenates were prepared from atrial or ventricular tissue and immunoblotted with anti-Kv1.5 (upper panels), anti-caveolin-3 (middle panels), or anti-caveolin-2 (lower panel) as indicated to the left of the blots (see Section 2) (RA – rat atrial lysate; RV – rat ventricular lysate; CA – canine atrial lysate; CV – canine ventricular lysate; LM – mouse *ltk*-cells).

the rat atrial and ventricular samples. As a control to ensure that the caveolin-2 antibody could detect protein in other cell systems, we probed extracts from mouse *ltk*-cells (LM lane in Fig. 1, bottom panel), as fibroblasts are known to express caveolin-2 [34].

3.2. Kv1.5 and caveolin-3 do not co-immunoprecipitate

Having established the presence of Kv1.5 and caveolins in the tissue lysates, co-immunoprecipitations were carried out to determine whether Kv1.5 physically interacts with caveolin-3 in these tissues (Fig. 2). Results from rat and canine atrium and ventricle are presented in the same manner as in Fig. 1, with the rat samples shown to the left (Fig. 2). As shown in Fig. 2A (upper panels), antibody to Kv1.5 efficiently immunoprecipitated Kv1.5 from both rat and canine atrial and ventricular tissue. However, antibody to caveolin-3 failed to co-immunoprecipitate Kv1.5, as did control reactions lacking a precipitating antibody (-Ab lanes). A similar result was obtained with the reverse experiment (Fig. 2A, lower panels); antibody to caveolin-3 clearly immunoprecipitated caveolin as shown in lanes 4 and 6 (left panels) and lanes 3 and 6 (right panels), but failed to bring down with them detectable levels of Kv1.5 in the rat or canine samples, as indicated by the lack appropriate bands in the lanes probed with the anti-Kv1.5.

To ensure that our protocol was effective for co-immunoprecipitation of proteins known to interact with Kv1.5 and caveolin-3 [12,35,36], we carried out a number of control experiments. In the first set of controls (Fig. 2B), immunoprecipitates of Kv1.5 were probed with an antibody to sarcomeric α-actinin and, as expected, a band corresponding to actinin was found in each of the rat and canine cardiac samples (Fig. 2B, upper panels). Similarly, antibody to caveolin-3 co-immunoprecipitated eNOS in the rat ventricle (left lower panel) and co-immunoprecipitated β-dystroglycan from canine atrial lysates (right lower panel). None of these proteins were detected in the antibody-free controls (Fig. 2).

3.3. Kv1.5 and caveolin-3 show minimal co-localization in deconvolved fluorescent images

Having demonstrated that Kv1.5 and caveolin-3 do not co-immunoprecipitate from cardiac myocytes, we investigated whether the channel is present in the caveolar domain, as the channel could localize to caveolae without directly interacting with caveolins. To test this possibility, we examined the distribution of caveolin-3 and Kv1.5 in myocytes using wide-field microscopy and deconvolution techniques. Fig. 3 shows representative examples of computer-deconvolved images of Kv1.5 and caveolin-3 immunolabeled rat (Fig. 3A) and canine

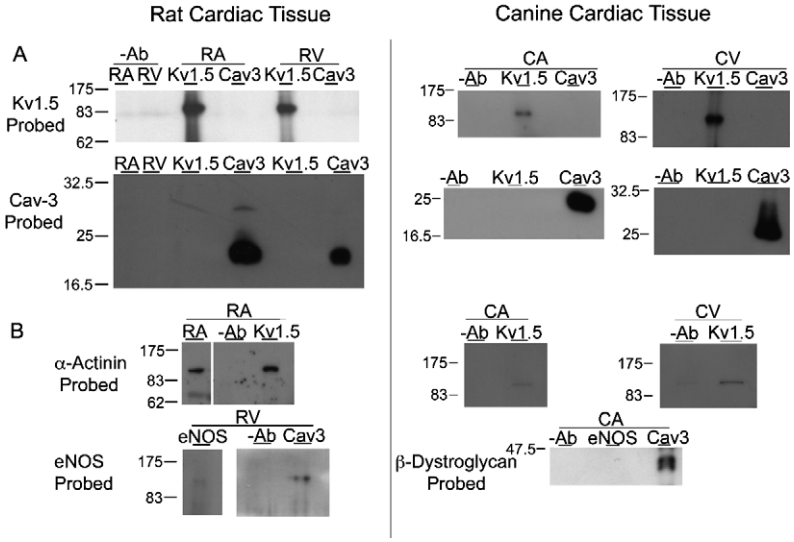

Fig. 2. Kv1.5 and caveolin-3 fail to co-immunoprecipitate from rat and canine atrial and ventricular homogenates. (A) Western blots of Kv1.5 and caveolin-3 immunoprecipitations from rat (left side of figure) and canine (right side of figure) cardiac tissue. The precipitating antibodies are indicated above each lane and the antibodies used to probe the blots are indicated to the left of the blots. The upper panels show immunoprecipitation of Kv1.5 but not co-immunoprecipitation with caveolin-3, while the lower panels show immunoprecipitation of caveolin-3 but not co-immunoprecipitation of Kv1.5. (B) Western blots showing positive controls of known co-immunoprecipitating proteins in heart. These include actinin with Kv1.5 (upper panels), eNOS with caveolin-3 (left lower panel), and β-dystroglycan with caveolin-3 (right lower panel). Other labels are as for Fig. 1.

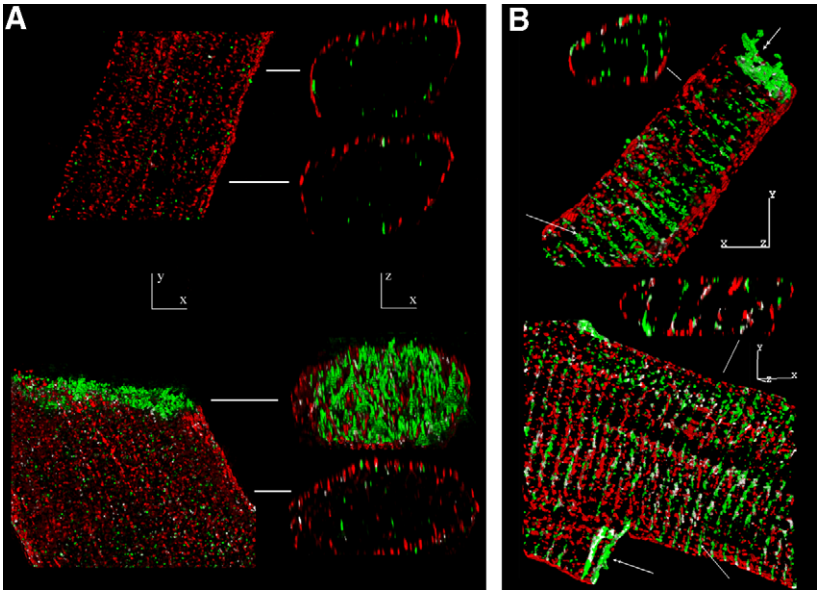

Fig. 3. Lack of co-localization of Kv1.5 and caveolin-3 in wide-field images of rat and canine cardiac myocytes. Rat (A) and canine (B) atrial (above) and ventricular (below) myocytes labeled with antibodies specific for Kv1.5 (green) and caveolin-3 (red), colocalized voxels are white. All of the images are 3D reconstructions, showing both *X*–*Y* and *X*–*Z* views of individual myocytes. (A) *XY* views are 6 μm thick, and their corresponding *XZ* views are 1 μm thick. Scale bar is 5 μm. The first *X*–*Z* view of the rat ventricular myocyte is at the level of the intercalated disc and highlights the intricate topology of this region as well as the higher levels of Kv1.5 staining. (B) *XY* view of the atrial myocyte is 7 μm thick, and the *XY* view of the ventricular myocyte is 3 μm thick. Their corresponding *XZ* views are 1 μm thick. Scale bar is 5 μm. The double-headed arrow points to the intercalated disc, the single arrow points to the *Z*-line.

(Fig. 3B) myocytes. Caveolin-3 is visualized with Alexa594 (red) and Kv1.5 with Alexa488 (green). In these 3D reconstructions, the resolution is calculated to be 122 nm in the *X*–*Y*-plane and 250 nm in the *Z*-plane (voxel size). In the rat atrial (top) and ventricular samples (bottom) it can be seen that caveolin-3 is highly expressed across the surface of the myocytes, as clearly confirmed in the cross-sectional images. In contrast, Kv1.5 expression is much lower, except at the intercalated disc, where Kv1.5 staining is very intense. In the ventricle, excluding the intercalated disc, Kv1.5 staining is most intense at the Z-line, adjacent to but distinct from the striated pattern of caveolin-3 staining; colocalization analysis revealed that 11 ± 4% of the voxels positive for Kv1.5 were also positive for caveolin-3 ($n = 4$) in these cells. In rat atrial myocytes (Fig. 3A), Kv1.5 weakly labeled the surface membrane and the interior of the cell, and only 8 ± 1% of voxels that showed Kv1.5 also showed caveolin-3 ($n = 5$). The findings in canine myocytes were similar. Caveolin-3 immunolabeling was also marked at the cell surface in atrial cells (Fig. 3B, upper panel), and at the surface and along Z-lines in canine ventricular myocytes (lower panel). Kv1.5 was also well expressed in both canine atrial and ventricular myocytes with strong surface and Z-line expression in both types of cell. Despite the widespread distribution of both proteins, colocalization in the atrial myocytes was poor at 12 ± 2%. Apparent colocalization was greater in the ventricle at 20 ± 3% ($P < 0.02$). Values are means ± S.E.M., with an *n* of 5 for each cell type.

3.4. Immuno-EM confirms that Kv1.5 and caveolin-3 are differentially distributed in cardiac tissue

To examine the distribution of Kv1.5 and caveolin-3 in cardiac tissue at a higher resolution than the 122 nm × 122 nm (*X* and *Y*) by 250 nm (*Z*) possible using the deconvolution technique, we immunogold labeled ~70 nm thick Tokuyasu sections (see Section 2) of rat atrial and ventricular tissue and examined them by electron microscopy (Fig. 4). In these samples, caveolin-3 was immediately detectable as 10 nm gold particles distributed both at the cell surface and immediately below in flask-like structures (Fig. 4A). In contrast, Kv1.5 was labeled with 5 nm gold particles and more rarely seen (identified by arrows in panels A–C). Despite the low density of Kv1.5 staining in both atrial (Fig. 4A, B) and ventricular samples (Fig. 4C), Kv1.5 was well separated from caveolin-3 labeling. In none of the EM sections illustrated was coincident labeling of the two proteins found. Overall, even Kv1.5 and caveolin near-juxtaposition was extremely rare; 5 and 10 nm gold particles were found within 10 nm of each other in less than 1% of the sections examined. However, it is important to note that Kv1.5 and caveolin, while labeling distinct domains, could be found within 100 nm (i.e., within the voxel size for wide-field microscopy) in about 20% of TEM images positive for both proteins (as seen in Fig. 4A, B).

The TEM image of an atrial section (Fig. 4A) illustrates a segment of surface membrane showing at least one clear caveolus, a segment of a *Z*-line, surface and internal Kv1.5 staining possibly corresponding to SR localization or as vesicular cargo. Fig. 4B shows a lateral membrane region rich in caveolae with two 5 nm gold particles indicated by the arrow in the enlargement of the boxed region. The ventricular image (Fig. 4C) illustrates an intercalated disc region. The predominant labeling of Kv1.5 found along the *Z*-lines and at the intercalated discs confirms the observations made using fluorescence microscopy (Fig. 3).

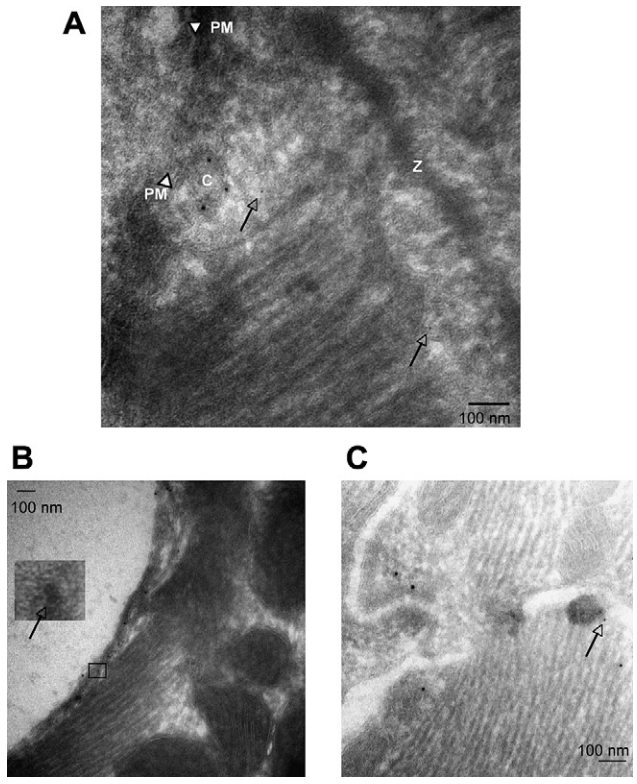

Fig. 4. Kv1.5 and caveolin-3 do not co-localize in immuno-EM images of rat cardiac myocytes. Images are of rat atrial (A and B) and ventricular (C) tissue. Cryosections (70 nm) were immunogold labeled for Kv1.5 (5 nm gold; indicated by black arrows) and caveolin-3 (10 nm gold). Boxed region in (B) is shown at higher magnification in the inset. Image in (C) shows a region through the intercalated disc. Other than in the inset, scale bars represent 100 nm (In (A): PM, plasma membrane; *Z*, *Z*-line; C, caveolus).

3.5. *Kv1.5 sediments independently from caveolin-3 in sucrose gradient fractionations*

Caveolae exist as a subtype of lipid rafts; caveolin-1, for example, sediments in the lipid raft fraction in sucrose gradients [37]. In order to examine whether the channel could be biochemically localized to rafts, be they caveolar or not, membrane fractions from both HEK293 cells stably expressing Kv1.5 and from rat ventricular tissue were solubilized in 1% Triton X-100 at 4 °C and then fractionated in a sucrose step gradient. Twelve 1-ml fractions were removed from the top of the gradient and samples from each fraction were run on a denaturing gel. The light buoyant density fraction (Fraction 5) was identified using the raft marker flotillin (Fig. 5A lower panel) as our HEK293 cells express very little caveolin-1 (not shown). The transferrin receptor was used as a marker for non-raft associated fractions (Fig. 5A and B upper panels), and was found in fractions 9–12 as well as in the pellet from the fractionation (FP). Kv1.5 co-sedimented with the transferrin receptor in fractions 9–12, and was absent from fraction 5 in both the cultured cells (Fig. 5A, middle panel) and the cardiac tissue sample (Fig. 5B, lower panel). Immunoprecipitation reactions to concentrate channel protein confirmed that Kv1.5 is abundant in fraction ten but absent from the flotillin positive fraction five (data not shown).

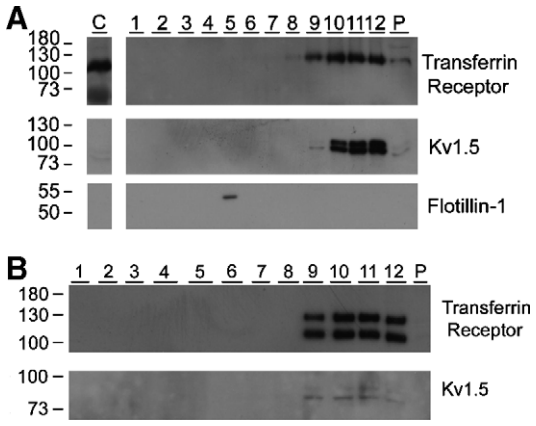

Fig. 5. Kv1.5 does not localize to the lipid raft fraction in HEK293 cells or rat ventricular tissue. (A) HEK293 cells stably expressing Kv1.5 and (B) Rat ventricular tissue were mechanically disrupted and the membrane fractions were separated by discontinuous sucrose gradient after solubilization in 1% Triton X-100 at 4 °C. Twelve fractions were collected starting from the top of the gradient and analyzed by Western blot. Flotillin-1 was used to delineate the raft fraction and the transferrin receptor the non-raft fractions. C is the supernatant from a $128000 \times g$ spin that pelleted the membranes and represents the cytosolic fraction. P is the soluble protein extracted from the sucrose gradient pellet with 2% SDS.

4. Discussion

In this study we have studied the localization of Kv1.5 by examining the direct physical interaction of the channel with the major caveolar coat protein, caveolin-3 using biochemical techniques, and the spatial distribution of the channel using wide field deconvolved and EM images of labeled myocytes. These experiments are the first to directly address the colocalization of Kv1.5 and caveolins in native cardiac tissues. In addition, we have examined the relationship of the channel and lipid rafts, membrane fractions characterized by a light-buoyant density and insensitivity to extraction by Triton X-100 at 4 °C. In isolated myocytes and cardiac tissue, the proteins did not co-immunoprecipitate (Fig. 2A) nor did Kv1.5 and caveolin-3 appreciably colocalize (Figs. 3 and 4), although interactions with other proteins known to associate with Kv1.5 or caveolin were detected (Fig. 2B). These observations were supported by fractionation results in which Kv1.5 was detected only in non-raft fractions in both HEK293 cells and in cardiac tissue (Fig. 5).

The relationship between Kv1.5 and caveolin has been controversial. Using co-immunoprecipitation experiments, Martens et al. [2] found no direct interaction between Kv1.5 and caveolin in cultured cells. However, using doubly transfected COS-7 cells overexpressing the two proteins, Folco et al., reported significant interaction between Kv1.5 and caveolin-3 [38]. And, using a similar over-expression system, Martens et al. [1] found that immature Kv1.5 copurifies with immunoisolated caveolae. Here, we have examined the phenomenon in native tissue in which the proteins are endogenously expressed, rather than in transfected heterologous cell lines with the attendant issues surrounding overexpression of non-native proteins. Thus, it would appear that Kv1.5 and caveolin-3 sort independently in cardiac tissue from the rat and dog. Whether the channel can interact with caveolins in other species or tissues remains an open question.

In addition to the caveolin-3 studies, we looked for an interaction of Kv1.5 with caveolin-2. However, while we were able to detect caveolin-2 in rat atrial and ventricular lysates (Fig. 1, bottom panel), we found no caveolin-2 in isolated rat cardiac myocytes despite repeated immunolabeling attempts under varied conditions (data not shown). Woodman et al. [8] similarly failed to find caveolin-2 in myocytes and reported that caveolin-2 expression is limited to the endothelium and endocardium. Our findings are consistent with their data; in similar experiments using canine tissue we were unable to detect caveolin-2 at all (Fig. 1). Perhaps caveolin-2 was absent in the tissue we employed or perhaps our result was due to the inability of the monoclonal antibody to recognize the canine protein, which is more diverged from human caveolin-2 than is the rat.

In their report of an association between Kv1.5 and immuno-isolated caveolae, Martens et al. [2] described an association of immature core glycosylated Kv1.5 with immuno-isolated caveolae in their mouse *ltk*-cells, but found that post-translationally modified Kv1.5 was absent from these caveolae. In our experience, cardiac myocytes lack significant amounts of the immature protein, as indicated by a single band migrating at approximately 83 kDa in cardiac lysate Western blots. This is apparent comparing the single Kv1.5 band in Fig. 1 to the doublet of mature and immature forms of the channel seen in HEK cells (Fig. 5 and [39]), suggesting that in native cells the channel is more efficiently processed. This lack of significant pools of immature channels may explain our findings that Kv1.5 and caveolin-3 did not co-immunoprecipitate or colocalize in cardiac myocytes (Figs. 2–4). It is possible that in heterologous over-expression systems some immature protein reaches the cell surface and associates with caveolae or, conceivably even, overexpression of the channel leads to an intracellular interaction with vesicles harboring caveolin. In mature cardiac myocytes, on the other hand, our data would indicate that neither process occurs to any significant extent.

The distribution of Kv1.5 in the myocytes is of interest, irrespective of its relationship to caveolin. In previous work with canine myocytes, we found that the results of Kv1.5 localization studies are very much dependent upon the anti-Kv1.5 antibody used [23]. The antibody employed here was developed by us, is highly specific to Kv1.5 [23] and has been used by others [40]. This antibody has enabled us to compare the distribution of Kv1.5 in rat and canine myocytes to that observed by others in rat [41], mouse [42] and human [43]. The observation most consistent across studies is that Kv1.5 staining is low on lateral membranes and *Z*-lines and enriched at the intercalated disc. This is true in rat, canine and human, while in mouse the labeling appears to be more generally at the cell surface and at *Z*-lines, at least in ventricular cells [42].

While expression at the cell surface is consistent with Kv1.5 function, it is not obvious why Kv1.5 should localize so strongly to the intercalated disk. It is difficult to envision a functional role for an ion channel in that structure. Interestingly, other channels have also been found to be largely localized to the intercalated disc, including Kv4.2 [41] and $Na_v1.5$ [44,45]. A sodium–hydrogen exchanger has also been localized to this domain [46]. The $Na_v1.5$ sodium channel resident at the intercalated disk has been suggested even to play a role in initiation and conduction of the action potential [44,45]. Thus, it is possible that ion channels are somehow functional in the intercalated disk. Alternatively, the intercalated disk may merely serve as a storage site for excess channels or, perhaps, these proteins play a structural role at this site. The finding of Kv1.5 staining at the *Z*-lines might also reflect internal stores of the channel or, perhaps, localization of the channel to T-tubules or T-tubule-like structures.

Unlike Kv1.5, caveolin largely localizes to the cell membrane in fluorescent imaging experiments. Very little Kv1.5 channel staining overlaps with the abundantly expressed caveolin-3 protein (Fig. 3A, B). Given the relatively low resolution of the florescence imaging system (calculated to be 122 nm in the *X*–*Y*-plane and 250 nm in the *Z*-plane), the 8–20% apparent colocalization seen under the light microscope at this voxel size is not strong evidence that the two proteins are associated, since results with electron microscopy showed a similar 20% of immunogold-labeled Kv1.5 and caveolin molecules lie within such voxel spaces yet are clearly separated (Fig. 4). These results highlight the complementary value of these two imaging techniques. While the TEM experiments greatly improved the resolution and enabled us to look more carefully at the channel distribution in relation to caveolin-3 and several ultra-structural elements, the fluorescent images gave a more general sense of staining that is impossible to appreciate when tightly focused on specific regions of the cell.

The TEM images showed sparse Kv1.5 staining and this is expected given the calculated channel density in rat atrium. Assuming a specific capacitance of 0.01 pF/μm^2 (average atrial myocyte capacitance of 40.7 pF and therefore a cell surface area of about 4070 μm^2), a maximal slope conductance of 103 pS/pF [47], a maximal open probability of 0.80, and a single channel conductance of 13 pS for Kv1.5, then we would expect to see ~1 channel per 10 μm^2. If we decrease the open probability to 0.5 then we would expect a channel in every 6.3 μm^2. These calculations would indicate that in each 6–10 μm length of surface membrane examined in the 70 nm thick EM sections, we would expect to see less than one channel. Depending on how much of the channel partitioned into each given section there is the possibility to label each subunit in the channel, which would result in up to four labels per channel, depending on the degree of steric hindrance. If the average thickness of a myocyte were 12 μm then we would expect that each myocyte would produce ~170 sections. From these numbers it would seem that the occurrence of functional channels in the lateral membranes is quite low especially given the apparent concentration at the intercalated disc region shown in the fluorescent images (Fig. 3). Therefore, it was entirely expected in the TEM images of immunolabeled myocytes that channel abundance was quite low. We have no way of calculating how many non-functional channels there may be, both at the surface and those in intracellular compartments, such as in early endosomes, which would be detected in the immunolabeling experiments but would not contribute to current density.

Given that we could find little evidence of Kv1.5 localization to caveolae, it was important to establish whether the channel partitioned into non-caveolar lipid rafts in our heterologous expression system (HEK293 cells) or in cardiac tissue. No Kv1.5 immunoreactivity was observed in the raft fraction from HEK293 cells or the rat ventricular sample; the majority of the channel protein clearly fractionated with the non-raft marker, the transferrin receptor (Fig. 5). Similarly, as stated earlier, Martens, et al failed to find mature, glycosylated Kv1.5 in the raft fraction of heterologous cells [2]. In addition, in further electrophysiological experiments, treatment of canine at-

rial myocytes with methyl-β-cyclodextrin, a drug that disrupts lipid rafts by depleting the cell membrane of cholesterol, resulted in a decrease in the instantaneous current (I_{TO}; underlain by Kv4.2) but had no obvious effects on the sustained current which is largely underlain by Kv1.5 [23] (data not shown).

Also inconsistent with an association of Kv1.5 with caveolae, we have shown that pretreatment of HEK293 cells with the actin-depolymerizing agent, cytochalasin D leads to a large increase in Kv1.5 surface expression [35]. It is known that surface caveolin-1 levels are decreased by disruption of the actin cytoskeleton in CHO cells, which, like HEK cells express caveolin-1 [48].

In summary, we have found that Kv1.5 and caveolin-3 fail to coimmunoprecipitate from, and reside in different locales in rat and canine cardiac myocytes and the failure to detect the channel in raft fractions, it seems likely that caveolae and lipid raft domains play little or no role in the localization of Kv1.5 in native adult cardiac myocytes.

Acknowledgements: This work has been supported by Grants to D.F. and E.M. from the Heart and Stroke Foundations for British Columbia and Yukon and from the Canadian Institute for Health Research, and by a Grant to D.V.W. from the National Institute of Health (NHLBI, 1RO1-HL-65412). We thank Paul Murray, Ph.D. for providing access to canine tissues, Changiz Taghibiglou, Ph.D. for his assistance and the raft isolation protocol, George Posthuma, Ph.D. for Tokuyasu protocols and EM advice, Qixia Yu and Garnet Martens for technical support in wide-field and electron microscopy, respectively, and David Steele, Ph.D. for editorial comments.

References

[1] Martens, J.R., Navarro-Polanco, R., Coppock, E.A., Nishiyama, A., Parshley, L., Grobaski, T. and Tamkun, M.M. (2000) Differential targeting of Shaker-like potassium channels to lipid rafts. J. Biol. Chem. 275, 7443–7446.

[2] Martens, J.R., Sakamoto, N., Sullivan, S.A., Grobaski, T.D. and Tamkun, M.M. (2001) Isoform-specific localization of voltage-gated K^+ channels to distinct lipid raft populations. Targeting of Kv1.5 to caveolae. J. Biol. Chem. 276, 8409–8414.

[3] Wong, W. and Schlichter, L.C. (2004) Differential recruitment of Kv1.4 and Kv4.2 to lipid rafts by PSD-95. J. Biol. Chem. 279, 444–452.

[4] Xia, F., Gao, X., Kwan, E., Lam, P.P., Chan, L., Sy, K., Sheu, L., Wheeler, M.B., Gaisano, H.Y. and Tsushima, R.G. (2004) Disruption of pancreatic beta-cell lipid rafts modifies Kv2.1 channel gating and insulin exocytosis. J. Biol. Chem. 279, 24685–24691.

[5] Bock, J., Szabo, I., Gamper, N., Adams, C. and Gulbins, E. (2003) Ceramide inhibits the potassium channel Kv1.3 by the formation of membrane platforms. Biochem. Biophys. Res. Commun. 305, 890–897.

[6] Li, S., Galbiati, F., Volonte, D., Sargiacomo, M., Engelman, J.A., Das, K., Scherer, P.E. and Lisanti, M.P. (1998) Mutational analysis of caveolin-induced vesicle formation. Expression of caveolin-1 recruits caveolin-2 to caveolae membranes. FEBS Lett. 434, 127–134.

[7] Galbiati, F., Engelman, J.A., Volonte, D., Zhang, X.L., Minetti, C., Li, M., Hou Jr., H., Kneitz, B., Edelmann, W. and Lisanti, M.P. (2001) Caveolin-3 null mice show a loss of caveolae, changes in the microdomain distribution of the dystrophin–glycoprotein complex, and T-tubule abnormalities. J. Biol. Chem. 276, 21425–21433.

[8] Woodman, S.E., Park, D.S., Cohen, A.W., Cheung, M.W., Chandra, M., Shirani, J., Tang, B., Jelicks, L.A., Kitsis, R.N., Christ, G.J., Factor, S.M., Tanowitz, H.B. and Lisanti, M.P. (2002) Caveolin-3 knock-out mice develop a progressive cardiomyopathy and show hyperactivation of the p42/44 MAPK cascade. J. Biol. Chem. 277, 38988–38997.

[9] Aravamudan, B., Volonte, D., Ramani, R., Gursoy, E., Lisanti, M.P., London, B. and Galbiati, F. (2003) Transgenic overexpression of caveolin-3 in the heart induces a cardiomyopathic phenotype. Hum. Mol. Genet. 12, 2777–2788.

[10] Li, S., Couet, J. and Lisanti, M.P. (1996) Src tyrosine kinases, Galpha subunits, and H-Ras share a common membrane-anchored scaffolding protein, caveolin. Caveolin binding negatively regulates the auto-activation of Src tyrosine kinases. J. Biol. Chem. 271, 29182–29190.

[11] Song, K.S., Li, S., Okamoto, T., Quilliam, L.A., Sargiacomo, M. and Lisanti, M.P. (1996) Co-purification and direct interaction of Ras with caveolin, an integral membrane protein of caveolae microdomains. Detergent-free purification of caveolae microdomains. J. Biol. Chem. 271, 9690–9697.

[12] Feron, O., Belhassen, L., Kobzik, L., Smith, T.W., Kelly, R.A. and Michel, T. (1996) Endothelial nitric oxide synthase targeting to caveolae. Specific interactions with caveolin isoforms in cardiac myocytes and endothelial cells. J. Biol. Chem. 271, 22810–22814.

[13] Lasley, R.D., Narayan, P., Uittenbogaard, A. and Smart, E.J. (2000) Activated cardiac adenosine A(1) receptors translocate out of caveolae. J. Biol. Chem. 275, 4417–4421.

[14] Fujita, T., Toya, Y., Iwatsubo, K., Onda, T., Kimura, K., Umemura, S. and Ishikawa, Y. (2001) Accumulation of molecules involved in alpha1-adrenergic signal within caveolae: caveolin expression and the development of cardiac hypertrophy. Cardiovasc. Res. 51, 709–716.

[15] Xiang, Y., Rybin, V.O., Steinberg, S.F. and Kobilka, B. (2002) Caveolar localization dictates physiologic signaling of beta 2-adrenoceptors in neonatal cardiac myocytes. J. Biol. Chem. 277, 34280–34286.

[16] Lasley, R.D. and Smart, E.J. (2001) Cardiac myocyte adenosine receptors and caveolae. Trends Cardiovasc. Med. 11, 259–263.

[17] van Deurs, B., Roepstorff, K., Hommelgaard, A.M. and Sandvig, K. (2003) Caveolae: anchored, multifunctional platforms in the lipid ocean. Trends Cell Biol. 13, 92–100.

[18] Nabi, I.R. and Le, P.U. (2003) Caveolae/raft-dependent endocytosis. J. Cell Biol. 161, 673–677.

[19] Isshiki, M. and Anderson, R.G. (2003) Function of caveolae in Ca^{2+} entry and Ca^{2+}-dependent signal transduction. Traffic 4, 717–723.

[20] Fedida, D., Wible, B., Wang, Z., Fermini, B., Faust, F., Nattel, S. and Brown, A.M. (1993) Identity of a novel delayed rectifier current from human heart with a cloned K^+ channel current. Circ. Res. 73, 210–216.

[21] Feng, J.L., Wible, B., Li, G.R., Wang, Z.G. and Nattel, S. (1997) Antisense oligodeoxynucleotides directed against Kv1.5 mRNA specifically inhibit ultrarapid delayed rectifier K^+ current in cultured adult human atrial myocytes. Circ. Res. 80, 572–579.

[22] Van Wagoner, D.R. (2000) Pharmacologic relevance of K^+ channel remodeling in atrial fibrillation. J. Mol. Cell. Cardiol. 32, 1763–1766.

[23] Fedida, D., Eldstrom, J., Hesketh, J.C., Lamorgese, M., Castel, L., Steele, D.F. and Van Wagoner, D.R. (2003) Kv1.5 is an important component of repolarizing K^+ current in canine atrial myocytes. Circ. Res. 93, 744–751.

[24] Nitabach, M.N., Llamas, D.A., Thompson, I.J., Collins, K.A. and Holmes, T.C. (2002) Phosphorylation-dependent and phosphorylation-independent modes of modulation of Shaker family voltage-gated potassium channels by Src family protein tyrosine kinases. J. Neurosci. 22, 7913–7922.

[25] Mason, H.S., Latten, M.J., Godoy, L.D., Horowitz, B. and Kenyon, J.L. (2002) Modulation of Kv1.5 currents by protein kinase A, tyrosine kinase, and protein tyrosine phosphatase requires an intact cytoskeleton. Mol. Pharmacol. 61, 285–293.

[26] Li, G.R., Feng, J.L., Wang, Z.G., Fermini, B. and Nattel, S. (1996) Adrenergic modulation of ultrarapid delayed rectifier K^+ current in human atrial myocytes. Circ. Res. 78, 903–915.

[27] Dupree, P., Parton, R.G., Raposo, G., Kurzchalia, T.V. and Simons, K. (1993) Caveolae and sorting in the trans-Golgi network of epithelial cells. EMBO J. 12, 1597–1605.

[28] Feron, O., Smith, T.W., Michel, T. and Kelly, R.A. (1997) Dynamic targeting of the agonist-stimulated m2 muscarinic acetylcholine receptor to caveolae in cardiac myocytes. J. Biol. Chem. 272, 17744–17748.

[29] Smythe, G.M., Eby, J.C., Disatnik, M.H. and Rando, T.A. (2003) A caveolin-3 mutant that causes limb girdle muscular dystrophy type 1C disrupts Src localization and activity and induces apoptosis in skeletal myotubes. J. Cell Sci. 116, 4739–4749.
[30] Eldstrom, J., Choi, W.S., Steele, D.F. and Fedida, D. (2003) SAP97 increases Kv1.5 currents through an indirect N-terminal mechanism. FEBS Lett. 547, 205–211.
[31] Scriven, D.R., Dan, P. and Moore, E.D. (2000) Distribution of proteins implicated in excitation–contraction coupling in rat ventricular myocytes. Biophys. J. 79, 2682–2691.
[32] Hohl, C.M. and Altschuld, R.A. (1991) Response of isolated adult canine cardiac myocytes to prolonged hypoxia and reoxygenation. Am. J. Physiol. 260, C383–C391.
[33] Slot, J.W., Geuze, H.J., Gigengack, S., James, D.E. and Lienhard, G.E. (1991) Translocation of the glucose transporter GLUT4 in cardiac myocytes of the rat. Proc. Natl. Acad. Sci. USA 88, 7815–7819.
[34] Scherer, P.E., Lewis, R.Y., Volonte, D., Engelman, J.A., Galbiati, F., Couet, J., Kohtz, D.S., van Donselaar, E., Peters, P. and Lisanti, M.P. (1997) Cell-type and tissue-specific expression of caveolin-2. Caveolins 1 and 2 co-localize and form a stable hetero-oligomeric complex in vivo. J. Biol. Chem. 272, 29337–29346.
[35] Maruoka, N.D., Steele, D.F., Au, B.P.Y., Dan, P., Zhang, X., Moore, E.D.W. and Fedida, D. (2000) α-Actinin-2 couples to cardiac Kv1.5 channels, regulating current density and channel localization in HEK cells. FEBS Lett. 473, 188–194.
[36] Sotgia, F., Lee, J.K., Das, K., Bedford, M., Petrucci, T.C., Macioce, P., Sargiacomo, M., Bricarelli, F.D., Minetti, C., Sudol, M. and Lisanti, M.P. (2000) Caveolin-3 directly interacts with the C-terminal tail of beta-dystroglycan. Identification of a central WW-like domain within caveolin family members. J. Biol. Chem. 275, 38048–38058.
[37] Sargiacomo, M., Sudol, M., Tang, Z.L. and Lisanti, M.P. (1993) Signal-transducing molecules and glycosyl-phosphatidylinositol-linked proteins form a caveolin-rich insoluble complex in Mdck cells. J. Cell Biol. 122, 789–807.
[38] Folco, E.J., Liu, G.X. and Koren, G. (2004) Caveolin-3 and SAP97 form a scaffolding protein complex that regulates the voltage-gated potassium channel Kv1.5. Am. J. Physiol. – Heart Circ. Physiol. 287, H681–H690.
[39] Eldstrom, J., Doerksen, K.W., Steele, D.F. and Fedida, D. (2002) N-terminal PDZ-binding domain in Kv1 potassium channels. FEBS Lett. 531, 529–537.
[40] Brunet, S., Aimond, F., Li, H., Guo, W., Eldstrom, J., Fedida, D., Yamada, K.A. and Nerbonne, J.M. (2004) Heterogeneous expression of repolarizing, voltage-gated K^+ currents in adult mouse ventricles. J. Physiol. 559, 103–120.
[41] Barry, D.M., Trimmer, J.S., Merlie, J.P. and Nerbonne, J.M. (1995) Differential expression of voltage-gated K^+ channel subunits in adult rat heart: relation to functional K^+ channels. Circ. Res. 77, 361–369.
[42] Trepanier-Boulay, V., St Michel, C., Tremblay, A. and Fiset, C. (2001) Gender-based differences in cardiac repolarization in mouse ventricle. Circ. Res. 89, 437–444.
[43] Mays, D.J., Foose, J.M., Philipson, L.H. and Tamkun, M.M. (1995) Localization of the Kv1.5 K^+ channel protein in explanted cardiac tissue. J. Clin. Invest. 96, 282–292.
[44] Kucera, J.P., Rohr, S. and Rudy, Y. (2002) Localization of sodium channels in intercalated disks modulates cardiac conduction. Circ. Res. 91, 1176–1182.
[45] Maier, S.K., Westenbroek, R.E., Schenkman, K.A., Feigl, E.O., Scheuer, T. and Catterall, W.A. (2002) An unexpected role for brain-type sodium channels in coupling of cell surface depolarization to contraction in the heart. Proc. Natl. Acad. Sci. USA 99, 4073–4078.
[46] Petrecca, K., Atanasiu, R., Grinstein, S., Orlowski, J. and Shrier, A. (1999) Subcellular localization of the Na^+/H^+ exchanger NHE1 in rat myocardium. Am. J. Physiol. 276, H709–H717.
[47] Van Wagoner, D.R., Kirian, M. and Lamorgese, M. (1996) Phenylephrine suppresses outward K^+ currents in rat atrial myocytes. Am. J. Physiol. – Heart Circ. Physiol. 271, H937–H946.
[48] Mundy, D.I., Machleidt, T., Ying, Y.S., Anderson, R.G. and Bloom, G.S. (2002) Dual control of caveolar membrane traffic by microtubules and the actin cytoskeleton. J. Cell Sci. 115, 4327–4339.